JPL XXXXXXXXXXX
EOS AIRS DRL XXX
ATBD-AIRS-01

Earth Observing System (EOS)

Atmospheric Infrared Sounder (AIRS)

AIRS Level 1C Algorithm Theoretical Basis

Yibo Jiang, Evan Manning, Hartmut H. Aumann and Denis A. Elliott

JPL

Margaret H. Weiler

Larrabee Strow and Scott Hannon

UMBC

Version 1.0
March 1, 2011

Jet Propulsion Laboratory
California Institute of Technology
Pasadena, California 91109-8099

Release Record

Version	date released	comments
1.0	March 1, 2011	Initial Release
2.0	March 10, 2012	Final Release

TABLE OF CONTENTS

1. Introduction and Review

1.1 AIRS Instrumentation

The Atmospheric Infrared Sounder (AIRS), launched aboard NASA's EOS Aqua spacecraft on May 4, 2002, is a grating array spectrometer having 2378 channels sensitive in the range 3.7 to 15.4 microns. The spectral resolution ($\lambda/\Delta\lambda$) is about 1200. A combination of a design philosophy having radiometric accuracy as a foremost goal, cooled and temperature-controlled spectrometer hardware (including most of the optics), and thorough pre-flight calibration have made the AIRS a superb instrument that produces very high quality radiance data [Strow *et al*., 2003]. The AIRS will have completed ten years in routine operations by the end of August 2012. The instrument remains healthy and it is hoped that it will continue to operate and produce high quality data for several more years. Such a long data record makes AIRS an excellent candidate for producing useful records for climate trend analyses. To maximize its utility as a source of climate data, any instrument must be capable of being accurately cross-calibrated with other instruments so that lengthy multi-instrument records may be generated.

Because AIRS is a grating array spectrometer, not a Fourier transform spectrometer, each of the 2378 channels is independent of the others, is separately calibrated, and has the potential for noise behavior that is different from the other channels—even neighboring ones. In fact, the noise behavior of a channel can change (or a channel could even stop functioning) suddenly, perhaps due to a radiation hit, without any other channel being affected. Channel variability in noise characteristics, if unaccounted for, complicates error estimates, noise estimates, and cross-instrument calibration.

In this document, we will describe the methodology and procedure that will produce cleaned-up AIRS spectra that can be conveniently used for instrument cross-calibration and studies of climate trends. The final output will be a prescription for producing Level 1C radiances that will become publicly available in a future version of the AIRS science product generation software (currently in Version 5) operating at the Goddard Earth Sciences Data and Information Services Center (GES DISC). Level 1A products contain raw detector counts. Level 1B consists of radiometrically calibrated radiances [Gaiser *et al*., 2003]. Both Level 1A and Level 1B have been produced since the start of routine instrument operations in September 2002. Level 1C will be cleaned up spectra, in which dead or unusually noisy channels have been marked and their radiances corrected or replaced using well-behaved correlated AIRS channels. Furthermore, the small gaps in the spectrum are filled in with reasonable values calculated from the same spectrum, and the discrepancies of overlapped channels between adjacent modules are corrected and the overlapped channels are removed.

1.2 The Motivation of Level 1C

An ideal spectrum should have the following properties:

1) All frequencies are included (at the design resolution) with no gaps and no overlapped spectral regions.
2) All channels have only Gaussian noise, so that far outliers do not interfere with integration over the pass band or interpolation during resampling.
3) Adjacent channels are truly independent measurements, with adjacent-channel correlations minimized.

4) The channel frequencies are fixed in time.

The AIRS instrument performance deviates from the ideal described above by small amounts. Actually, its in-flight performance has far exceeded its specifications, which were developed with temperature and humidity profile measurement in mind. The originally envisioned use of AIRS was for non-climate-related studies of atmospheric phenomena and for improved weather prediction. Because of its exceptional performance it is now being used for climate studies. AIRS climate data records can be improved if the deviations from ideal performance are accounted for.

AIRS, a grating array instrument, has seventeen detector modules spread across the focal plane. The hardware design was simplified by permitting small gaps in the frequency coverage between some modules, and small overlaps in coverage between others. These gaps and overlaps complicate the task of integrating the spectrum over the pass band to enable cross-instrument comparisons and calibrations.

Because of the large frequency range of the entire instrument, each detector module is made from different material having different properties, and unique read-out integrated circuits (ROIC). The shortwave modules include circuits to remove spikes resulting from radiation hits, while the spike resulting from radiation hits are very obvious in the longwave modules. Some channels exhibit non-Gaussian noise including “pops” (temporary changes in output level) and cold scene noise (scene-dependent noise larger at lower signal levels) [Weiler *et al*., 2005]. The AIRS detectors and their ROIC’s have different susceptibilities to radiation hits and to the slow build up of total radiation dosage throughout the mission. Thus, a channel that has exhibited very low noise for years can suddenly undergo a noise increase. It is also possible for a channel that has been affected by a radiation hit to recover after a period of hours or days. So noise can vary independently over time from channel to channel.

Each channel occupies its own physical space on the focal plane. That implies that slight changes in channel frequency can occur, due primarily to changes in temperature gradients within the spectrometer optical train. The AIRS spectrometer’s temperature is tightly controlled at one location by interactions between a radiator (cooling) and a heater. But small changes in internal gradients can occur and result in very small channel frequency shifts with time.

Grating array spectrometers, by their very nature, perform extremely well as far as point #3 above is concerned. However, the independence of the channels means that the other goals are not met automatically, and so must be handled explicitly. In this document, we describe each step towards a final Level 1C product that will fulfill the ideal. At first, we just handle point #2 above (variable and/or non-Gaussian noise). Points #1 and #4 will be handled last. Note that, because of the fact that the AIRS spectrometer is temperature controlled, point #4 (channel frequencies vs. time) has only a minor effect on AIRS data quality. The observed instrument frequency stability far exceeds the specification. But when the more stringent requirements for climate records are considered, it becomes clear that frequency shifts do need to be handled eventually.

Once “ideal” spectra have been produced, the use of AIRS data for many studies will be simplified and errors more easily estimated. Most importantly, it will be possible to cross-calibrate AIRS with other climate instruments more easily and reliably than that can be done today.

Figure 1 shows a typical L1B spectrum, where noisy or dead channels are indicated by the red dots at the bottom of the plot. The 17 modules and their location in the spectrum are also labeled in this plot. Of the 2378 AIRS spectral channels, about 58 have no response (dead), and an additional 34 channels (may change with time and location of the measurements) have more than 2K noise (compared to the nominal noise of 0.2K). The presence of these 92 channels is overemphasized in

Figure 1. The table 1 lists the gaps and overlapped regions of the spectrum which will be discussed in detail in session 4.

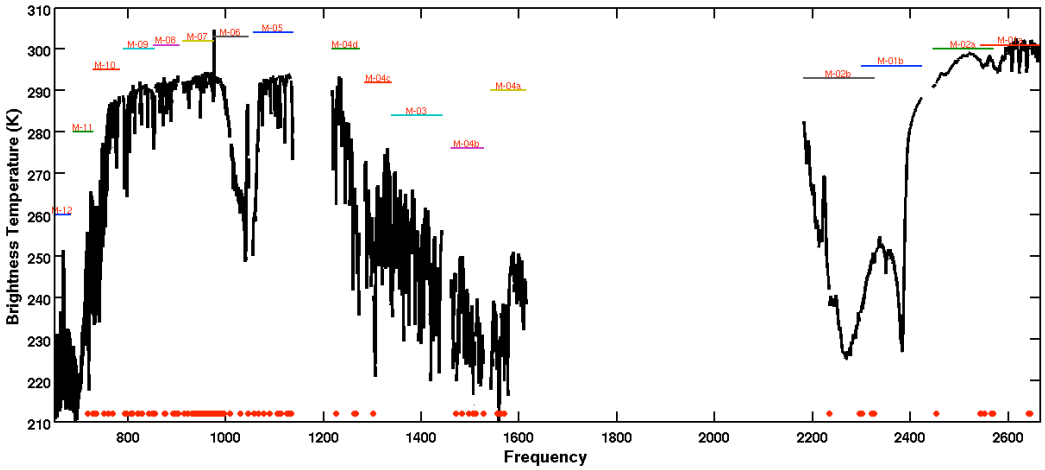

Figure 1. AIRS nighttime spectrum from January 1, 2006. The red dots at the bottom of the plot are indicators of dead or bad channels.

Table 1. AIRS Spectrum Gaps and Overlapped Regions

Type	Frequency Range (cm^{-1})	Comments
Gap	681.99-687.60	
	781.88-789.26	
	903.78-911.23	
	1046.20-1056.07	
	1136.63-1216.97	
	1272.59-1284.35	
	1443.07-1460.27	
	1527.00-1541.10	
	1613.86-2181.49	Large gap (will not be filled)
	2557.41-2558.53	
Overlap	727.83-728.36	M-11/M-12
	851.20-852.72	M-08/M-09
	973.48-974.63	M-06/M-07
	1337.64-1339.18	M-03/M-04c
	2301.72-2320.79	M-01b/M-02b
	2545.19-2565.21	M-01a/M-02a

The L1B spectra have four quality issues which can be addressed with the L1C software:

1. The radiances in L1B are correct, but the current frequencies may vary by up to 5 ppmf from the nominal frequencies due to diurnal and seasonal effects (Figure 2). The true frequencies are known to within 1 ppmf. The difference between the nominal and the actual frequencies causes errors in the interpretation of the radiances, which are very small compared to the random noise, but if ignored can produces artificial trends of as much as 10 mK/year in some channels.

2. AIRS has 2378 channels, but around 100 of the channels are "bad". We define "bad" as having NEDT>2K at the reference temperature of 250 K. The median NEDT at 250 K is 0.2 K. About 60 of these 100 channels were already dead (with -9999 value assigned in radiance) during prelaunch testing.
3. There are small gaps between the modules. This does not include the large gap from 1614 cm^{-1} to 2181 cm^{-1} which skips the shortwave part of the water band.
4. The channel sequence is not increasing monotonically in the overlapped regions.

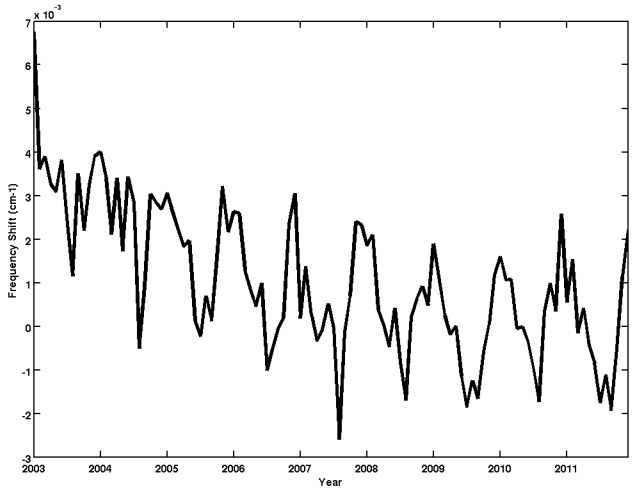

Figure 2. Monthly averaged AIRS instrument nighttime frequency shift in cm^{-1} from 2003 to 2011 in latitude range from -10 degree to 10 degree. (Larabee, what about the spike in January 2003?)

The issues in items 2 through 4 make it more difficult to uses AIRS L1B data for band-integrated comparisons with lower resolution sounders. The L1C product will address these three items as listed below.

1. Eliminate all overlap channels. The information about overlap is carried in the Cij flags.
2. Create a L1C AIRS nominal frequency set by using the grating model to define the frequencies of channels in the gaps. This is done by making the arrays in the model a little longer than the actual arrays. At this time we do not propose to fill the shortwave water band gap (1614 cm^{-1} to 2181 cm^{-1}).
3. Fill in all "bad" channels and the newly created gap filling channels with information from the good channels using Principal Component Analysis (PCA) and PCA reconstruction methods. Write the nominal (fixed) and actual channels frequencies into the L1B and L1C products.

The L1C AIRS nominal frequency array is monotonically increasing with no gaps and the L1C spectra have no bad channels. The RTA is valid for all channels that are not gap filled. Since the L1C spectra are essentially Nyquist sampled, they can be shifted by small amounts from the nominal frequency, without changes to the SRF or RTA and with no significant radiometric error using interpolation.

2. Spectrum Cleaning

This section describes the spectrum cleaning algorithm and its implementation. Test results are shown and then reconstruction differences are used to explore noise and spatial characteristics of the AIRS Level-1B product. The major steps in the spectrum cleaning process are:

- Identification of obviously bad channels.
- First-order replacement of these bad channels using the buddy system. This step is required or else the PCA diverges.
- PCA reconstruction of the spectrum and replacement of the bad channels.
- Scan the spectrum for outliers based on PCA reconstruction and identify noise spikes.

2.1 Dead or Noisy Channel Detection

For each observation, typically about 110 of 2378 channels are marked for replacement and others are excluded from use in replacing other channels. This process generally relies on noise levels, error flags, and radiances from the Level-1B product, so in theory different channels could be selected for replacement in each granule, but in operations we see mostly the same channels, including ~50 permanently dead or noisy from launch through the first 10 years of operations. An additional seven channels are marked permanently bad because they have been unusable since the launch of the AIRS instrument but are not always flagged as bad in the Level-1B product. These include 5 channels that are cross-wired, so they actually have low noise, but they do not observe the spectral region they were intended to.

Channel replacement is required whenever:

1) NEdT at 250 K scene temperature exceeds a threshold (currently 2.0 K) or NEdT is negative (indicating noise could not be characterized).
2) L1B provides no radiance value.
3) L1B CalFlag indicates a problem with gain or offset calculations, bad telemetry, or a “pop” event. Only pop events are common.
4) Channels are on a list of permanently bad detectors.

Channels are not replaced but are excluded from use in replacing other channels whenever:

1) NEdT at 250 K exceeds 1.0 K.
2) Observed radiance is negative.
3) AB_State from the current channel properties file marks the channel lower quality with state > 2.

The median NEDT at the reference temperature of 250 K is 0.2 K. The further detection of "bad" or "noisy" channels with the help of principal component analysis will be discussed later.

2.2 The Night-Time Clear-Sky Training Set

While the AIRS spectrum consists of 2378 independent spectral channels, the information content of the spectrum as a whole is much less. For all AIRS channels, there exist other AIRS channels

that are radiometrically similar. We can therefore replace the radiance of known bad or noisy channels with ones computed using these approximately equivalent channels or "buddies".

We prefer to select buddies for each channel by finding channels with similar statistics over a representative set of observed spectra. However, for our 7 permanently bad channels and about 100 others that are dynamically bad on the day used for this set, we can't do this. So these channels are first replaced using synthetic (simulated) spectra, then we can produce a training set with all channels good for training the final buddy replacement list and the principal component step.

The first training set is derived from AIRS night-time clear-sky spectra model simulation by UMBC radiation transfer model with 49 climatology spectra at satellite zenith angles 0, 10, 20, 30, 40, 50 degrees. Some of the spectra are shown in Figure 3.

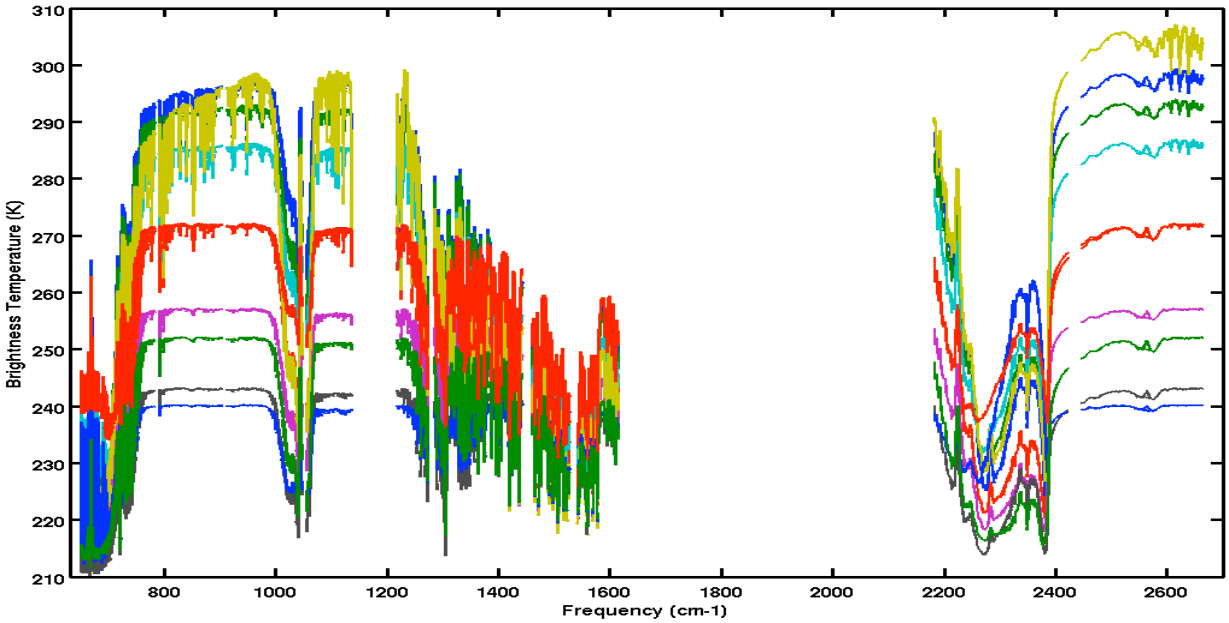

Figure 3. Examples of night-time clear-sky training sets.

2.3 The Global Training Set

The second training set (Figure 4) uses real AIRS spectra observed on January 1, 2008. There are 21,502 profiles in this training set, and they include day-time and night-time spectra, cloudy and dust cases. This was the largest number of samples in the training set that the PCA training algorithm could accommodate. The spectra were selected such as to represent all the factors that may affect the measurement. Each of the 21,502 spectra was cleaned and filled by the first set "buddy" replacement process. Some of the spectra are shown in Figure 4. This training set was used to find the new set of "buddies" which will be used in L1C process, and create the eigenvectors used for the detection and replacement of bad-channels by the Principal Component Analysis method [Jolliffe, 1986]. It was originally thought that any day would be equally good, because winter, summer, etc. conditions all will be encountered somewhere on the globe. But January 1st is near the start of northern winter, so this training set lacks the coldest cases, such as those seen in Antarctica in the coldest parts of southern winter. Evidence of this is shown below in figures 10-15.

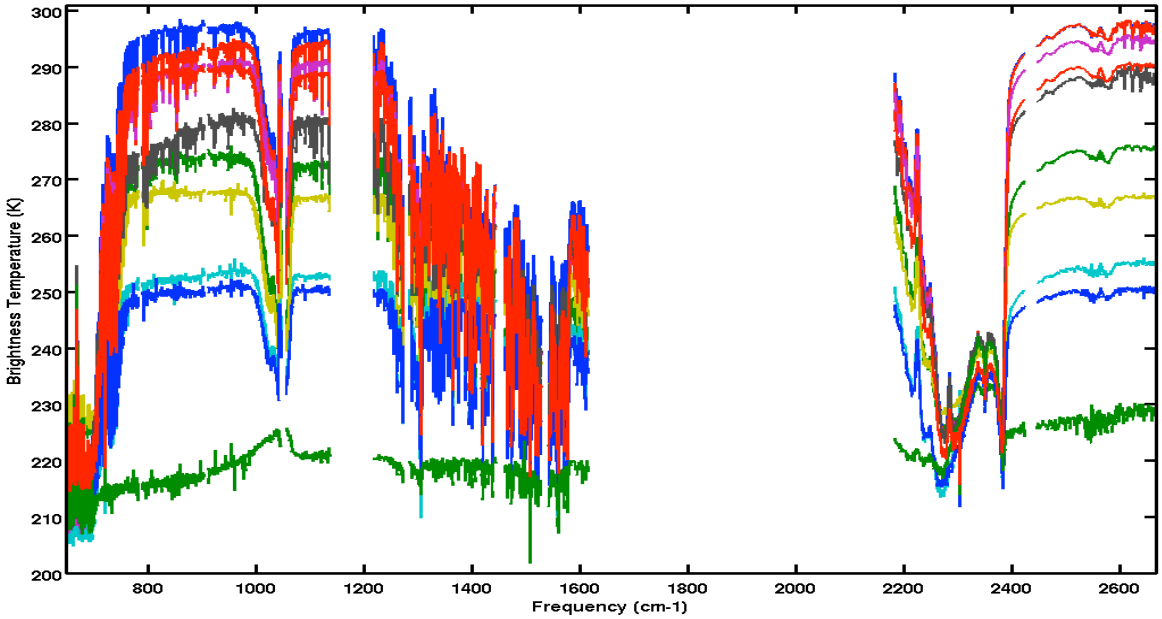

Figure 4. Example of second training sets.

The first step in selection of profiles for inclusion in the training set was to evaluate the median brightness temperature (BT) for each of the 17 detector module for each spectrum. See the Level-1B ATBD for more information on detector modules. Then the median of those medians was calculated as the overall median BT for the spectrum. The key parameters for distinguishing profiles were:

1) overall median BT
2) Delta BT between module M-12 (649-682 cm^{-1}) BT and overall median BT
3) Delta BT between module M-01b (2300-2422 cm^{-1}) BT and overall median BT
4) Delta BT between module M-01a (2546-2665 cm^{-1}) BT and overall median BT
5) Delta BT between module M-02a (2446-2564 cm^{-1}) BT and overall median BT
6) Delta BT between module M-04d (1217-1272 cm^{-1}) BT and overall median BT

6-dimensional bins were created by dividing each parameter into intervals:

1) overall median BT: 2K bins
2-5) delta M-12 through delta M-02a: range of values encountered is divided into 12 equal bins
7) delta M-04d: range of values encountered is divided into 8 equal bins

Then from each non-empty bin, one spectrum was selected at random. Assuming the overall median BT covers a span of about 100 K, this gives 50*12*12*12*12*8 ~= 8 million bins, but most combinations are empty.

2.4 Buddy-System Algorithm

In order to fill in the bad channels with reasonable values ("buddies") from the same spectrum, the most correlated channels (minimum standard deviation) are found based on the training set. The brightness temperature of the bad channel is then replaced by the brightness temperature from the most correlated channels. The correlated channel replacement list is calculated based on the following formula (1) which calculates the averaged deviation from the channel to be filled. Note that the "buddy" channels always come from the same detector module (Figure 1) as the channel that is being replaced.

$$\delta T(k,j) = \sqrt{\frac{1}{n}\sum_{i}^{n}(T_{ij} - T_{ik})^2} \qquad (1)$$

n: number of spectra in the training set
i: spectrum index, range from 1 to n;
j: channel number range from 1 to 2378;
k: channel to be filled range from 1 to 2378

T represents the brightness temperature in formula (1), *i* is the spectrum index in the training set, *j* is the replacement channel number and *k* is the channel number to be filled. $\delta T(k,j)$ represents the averaged deviation of each individual channel *j* to the filled channel *k*. For each channel *k*, $\delta T(k,j)$ values are sorted in the ascending order and the first 100 *j*s with the least deviations from channel *k* are selected and will be used to replace or fill the bad channels. This process is repeated for 10 15-Kscene brightness temperate ranges from [220, 235) to [355 ,370) K. The resulting 100 *j*s (integer array size 2378x100) and the associated deviations (double array size 2378x100) and biases are stored in a lookup table which will be used in the later process.

The brightness temperature of the channel to be filled or replaced then is the average of the four best correlated of the useable channels weighted by the deviations from the filled or replaced channel. In level 1C implementation, the four most correlated channels are used in the final calculation of the brightness temperature T_k of the replaced channels (Formula 2).

$$T_k = \frac{\sum_{j}(T_j + fB_r(k,j))\dfrac{1}{\delta T_r(k,j)}}{\sum_{j}\dfrac{1}{\delta T_r(k,j)}} \qquad (2)$$

j: channel number range from 1 to 2378;
k: channel to be filled range from 1 to 2378
r: brightness temperature range from 1 to 10
B: brightness temperature bias
f: bias scale factor

The use of a bias allows us to find much better matches than otherwise, but there is a catch. The degree of bias between neighboring channels is highly scene dependent: the more clouds, the less spectral contrast. Therefore, for each channel to be replaced and in each spectrum, we first determine a bias scale factor *f*. *f* is selected from among 9 possible values {0.00, 0.25, 0.50, 0.75, 1.00, 1.25, 1.50, 1.75, 2.00} by finding the value that minimizes the penalized standard deviation of the candidate fill values $T_j + fBr(k,j)$. The penalty function requires that the standard deviation be 4x smaller for the extreme bias scale factors of 0.00 and 2.00 than for the nominal value of 1.00, which makes the process favor using the nominal value.

Figure 6 shows a typical AIRS spectrum after the "buddy-system" replacement of dead or noisy channels. All visible outliers are suppressed and reasonably good values are provided for missing channels. Errors of 1-5 K are still important but not obvious on this scale, so we demonstrate the further improvements made by PCA in figure 8 below and then characterize the final cleaned product in section 2.6.

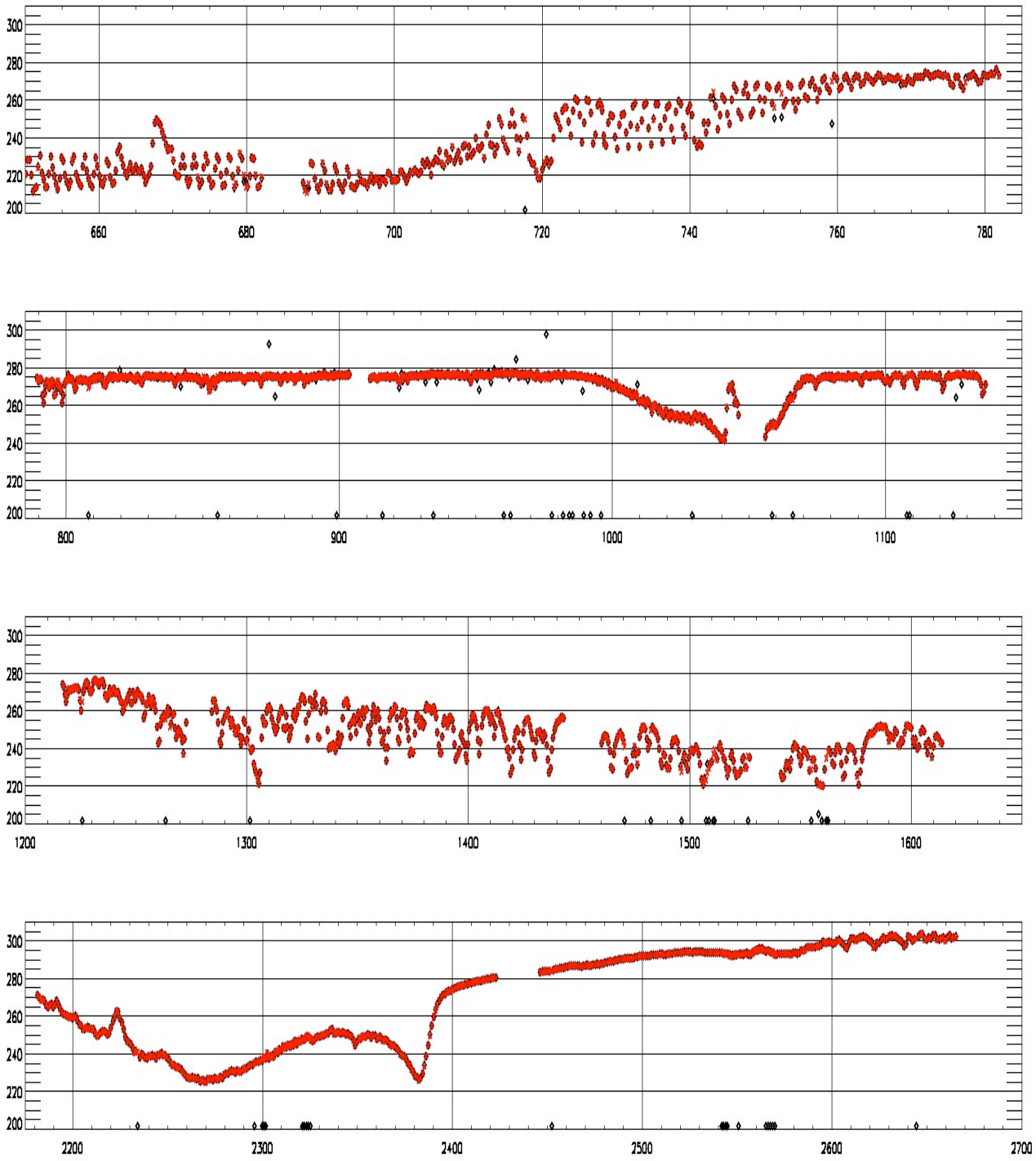

Figure 6. A typical AIRS spectrum after the first pass "buddy-system" replacement of dead or noisy channels. The black diamond symbol represents the original L1B spectrum and the red circle is the cleaned spectrum. Diamonds along the bottom of the spectrum are channels for which the L1B value was out of range or L1B did not provide a value.

2.5 Principal Component Analysis and AIRS Spectrum Reconstruction

Principal component analysis (PCA) involves a mathematical procedure that transforms a number of (possibly) correlated variables into a (smaller) number of uncorrelated variables called principal components. PCA is a simple, non-parametric method of extracting relevant information from complicate data set. Any data can be expressed as linear combinations of eigenvectors, where the first principal component (associated with the first eigenvector) accounts for most of the variability in the data, and each succeeding component accounts for remaining variability. The real spectrum training set is used to create the fixed set of eigenvectors. The first four major principal components and their eigenvalues of the training set are shown in Figure 7. The eigenvalues fall sharply, and the first twenty components account for over 99% of the signal. The number of components used to reconstruct the spectra increases, the reconstructed spectra will increasingly match the observed spectra, eventually including noise artifacts. Since we use the PCA reconstructed spectrum for noise detection, we choose 400 components in our PCA reconstruction scheme.

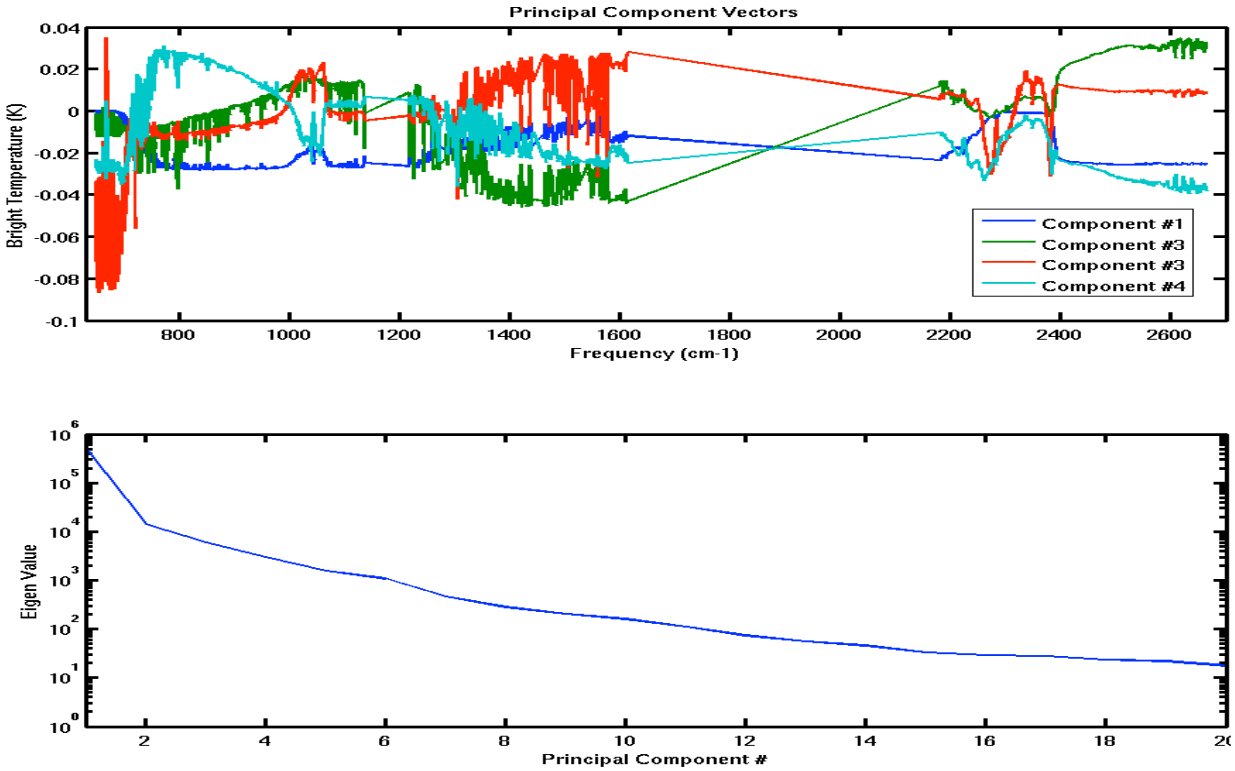

Figure 7. Principal component analysis of the training set for the first four components (top panel) and the eigenvalues for the first twenty components (bottom panel).

The observed spectrum T can then be reconstructed from the PCA using formula (3) where T represents the reconstructed brightness temperature, E^T is the transposed eigenvector, T_0 is the original spectrum, and $\overline{T}_T$ represents the average of the training set.

$$T = E^T T_0 + \overline{T}_T \tag{3}$$

Once a spectrum has been cleaned by the "buddy-system" replacement, the principal component analysis is used in order to further detect and correct the cleaned spectrum.

At the 100+ K scale of Figure 6, even the buddy system replacement looks perfect, but by zooming in we can observe the additional accuracy provided by the PCA step. Figure 8 shows a close-up of the 2290-2330 cm^{-1} spectral region of the same spectrum shown in Figure 6. Now in addition to black diamonds for the raw L1B spectrum and red Xs for the buddy replacements we have green +s for the PCA replacement. All good channels in L1B are not replaced and so have the same values for all 3 sets. 2300-2326 cm^{-1} is an "overlap" region where detectors from two detector modules observe almost the same frequencies and also where there are several bad detectors. The long red and green line segments connect the ends of the modules and make it easy to see the extent of the overlap region. Several channels at the ends of the modules (2300-2302 cm^{-1} and 2321-2325 cm^{-1}) are marked bad and replaced. For all of these channels the green PCA replacement values are more similar to values from good detectors in the other band than are the red buddy-system values. There is also one odd point at 2302.5 cm^{-1} where the two replacement values agree quite closely but disagree with the observation from the other band by over 1 K. The specific cause of this is not known, but this magnitude of error is within expectations.

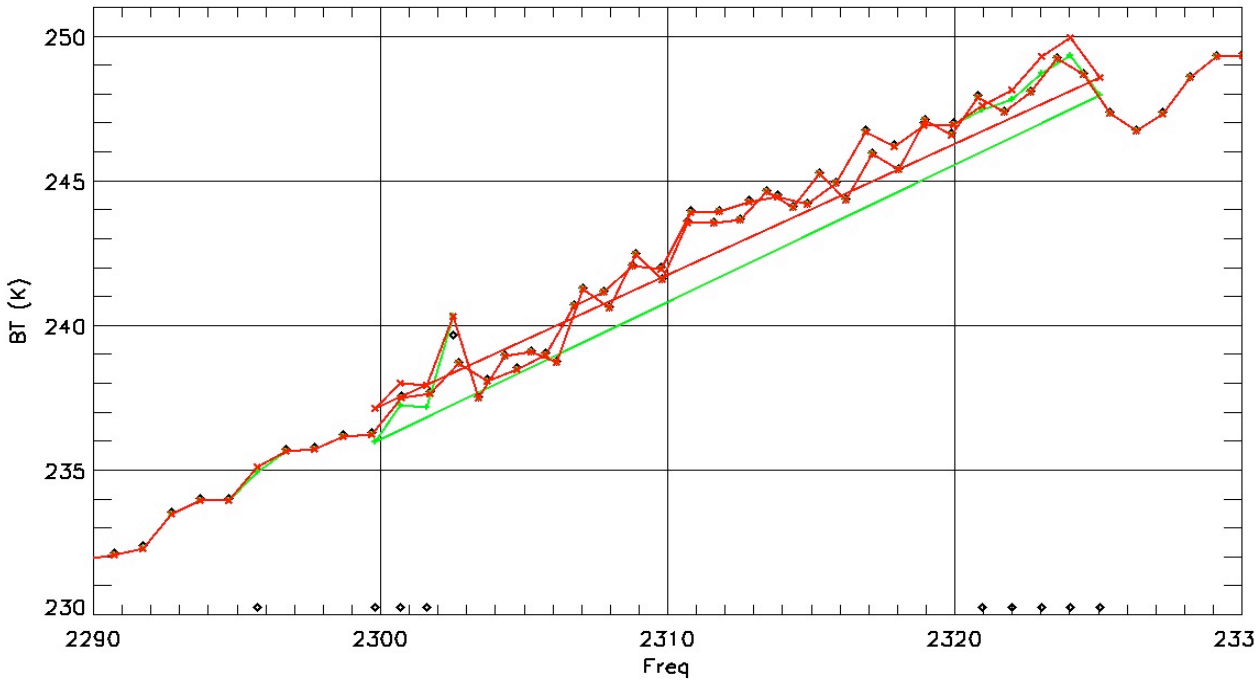

Figure 8. Close-up of buddy system and PCA replacement values in an overlap region. Black diamonds: L1B. Red Xs: Buddy system. Green +s: PCA.

2.6 Algorithm Validation

AIRS spectra themselves are the great source for the validation of the spectrum cleaning algorithm. For this test we ran all 240 granules for 2007-09-06 ten times, each time knocking out every 10^{th} channel from a different starting point. Then all of the replacement values were combined into a single spectrum for each observation. This spectrum is then compared to the actual observed Level-1B spectrum in order to evaluate the filling algorithm. This is a real stress test because where approximately 5% of channels are normally filled because of static or dynamic problems, now 15% of channels are replaced at once. Results shown include only

channels with reported noise level <= 0.6 K and only scenes where the L1B brightness temperature is at least 220 K.

Figure 9 shows the bias (black) and standard deviation (blue) by channel over the full day of data. The results are excellent, with bias almost always within +/- 0.1 K and std dev rarely much larger than the noise level. Even the outliers have bias under 1 K and std dev under 1.5 K, very good for the purposes of L1C.

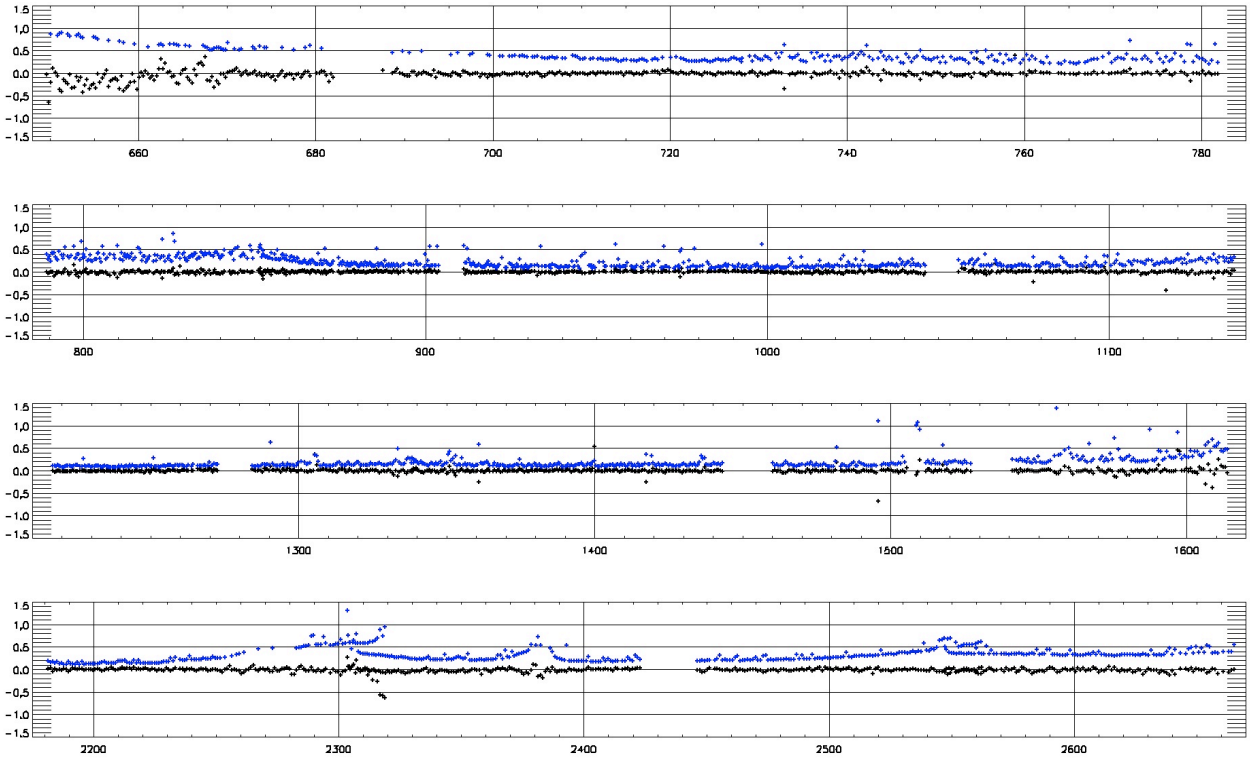

Figure 9. Bias (black) and standard deviation of reconstruction error (K) as a function of frequency (cm^{-1})

We can investigate this further by dividing the globe into 6 latitude zones. Figures 10 (bias) and 11 (standard deviation) give statistics by zone. From about 649-700 cm^{-1} we see a cold bias in the tropics, and throughout the spectrum but especially in the shortwave region from 2300-2660 cm^{-1} we see enhanced noise in the Antarctic. The enhanced noise may be caused by a lack of austral winter cases in the training set or might just be an artifact that noise levels in brightness temperature units get larger as scenes get colder.

In any case, the results are still excellent with all biases within +/- 1.5 K and standard deviation almost always in this range.

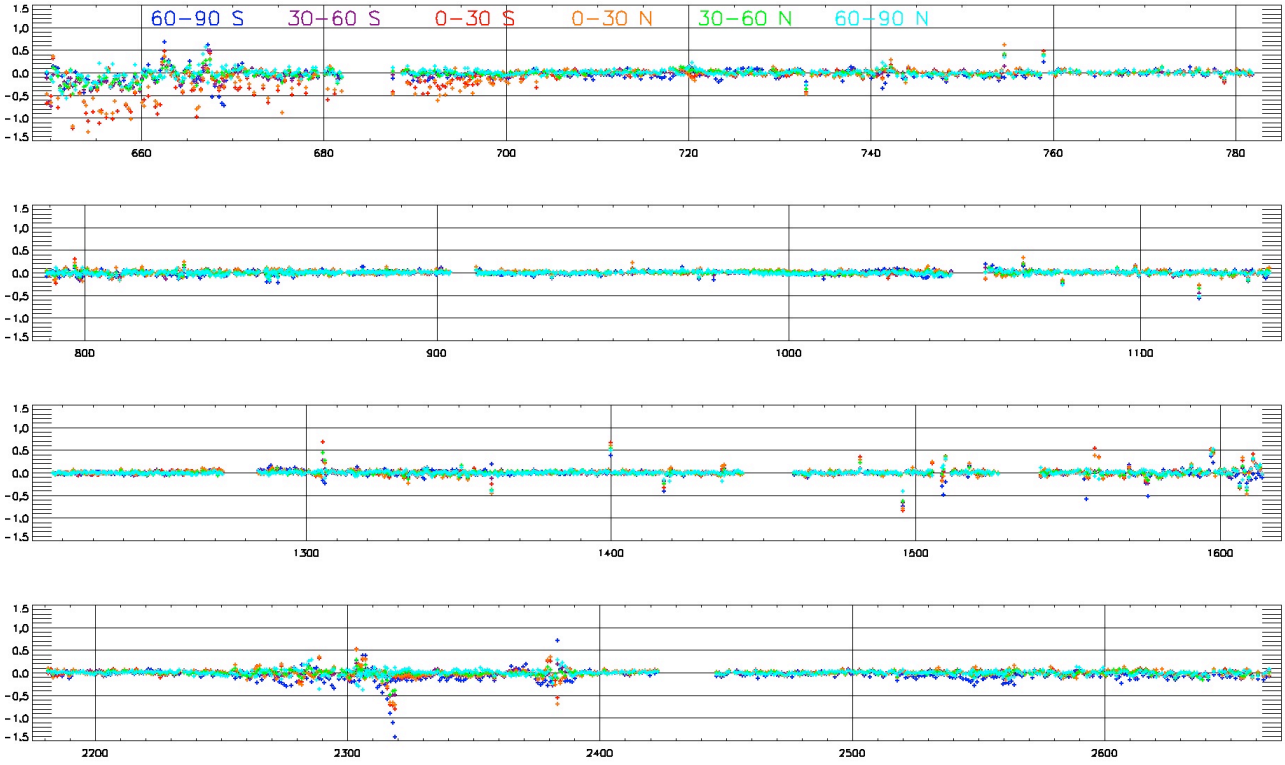

Figure 10. Bias of reconstruction error (K) as a function of frequency (cm^{-1}) by latitude zone.

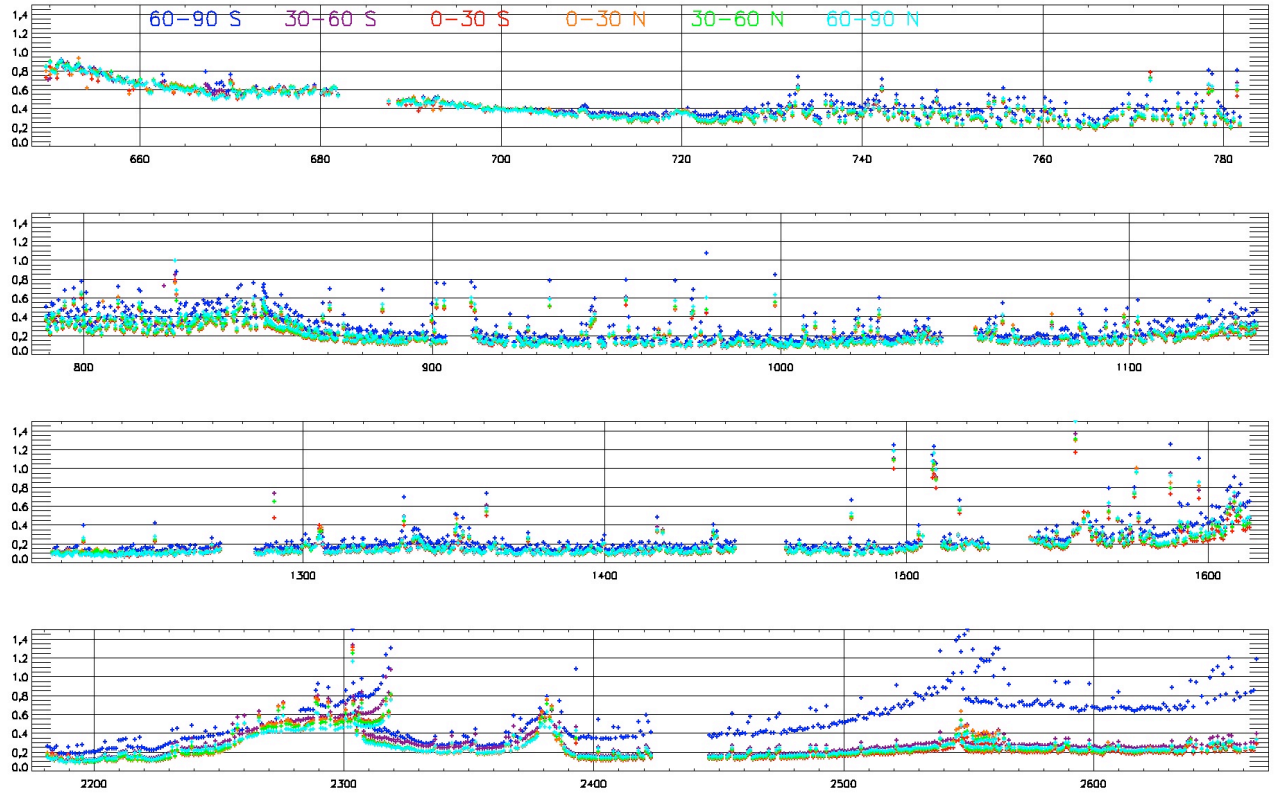

Figure 11. Standard deviation of reconstruction error (K) as a function of frequency (cm^{-1}) by latitude zone.

We can also look at histograms of the bias and standard deviation of per-granule reconstruction error for the full day. Figures 12 and 13 show that even at the granule level, outliers are extremely rare. There is evidence in figure 12 of a small cold bias overall with a magnitude << 0.1 K.

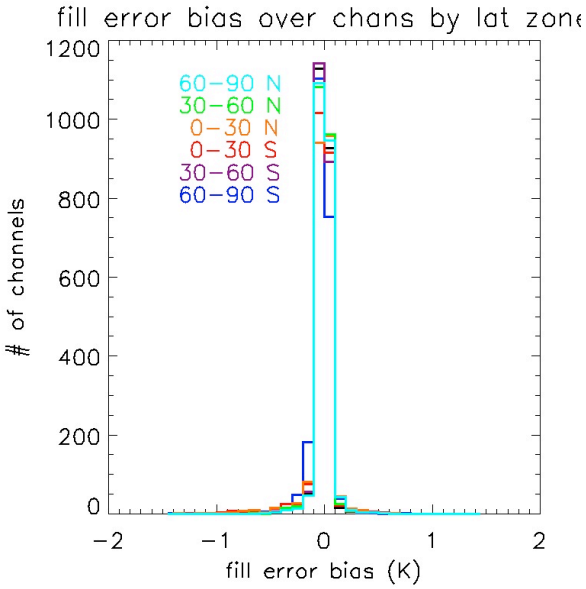

Figure 12

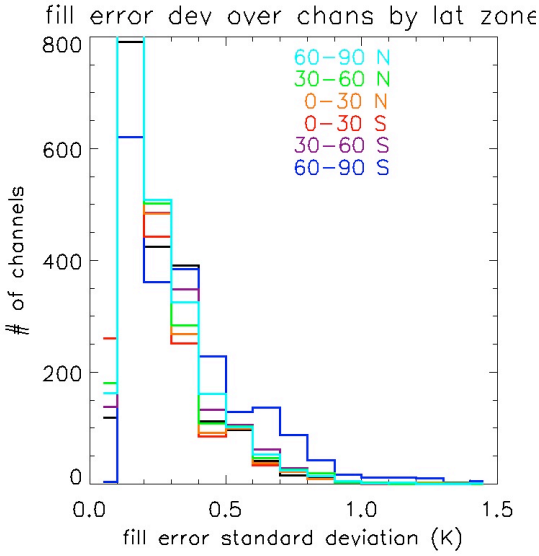

Figure 13

2.7 Using PCA reconstructed radiances to explore the quality of raw Level-1B

PCA provides a great tool to investigate misbehaving channels, channels that are not replaced by the cleaning process detailed above, but show significant differences between the observed Level-1B radiances and the principal component reconstruction of the same channel. It may also (optionally) be used to dynamically flag and/or replace problem channels.

For this analysis we again processed all 240 granules of 2007-09-06. This time we produced an output that cleaned all channels with PCA reconstructed values. For each granule/channel combination we checked for cases where cleaning was not performed by the nominal Level-1C but the difference between the observed and reconstructed radiances were significant. The criterion for significance is that at least one of the 135*90=12150 spectra has both a difference in BT units of at least 5 K and in radiance units of at least 5.7 times the noise level (5.7 sigma gives 1-in-100-million false positives assuming Gaussian noise. Over all 2378 channels * 12150 spectra, that works out to one false positive per 3-4 granules.)

The problem of Antarctic winter cases discussed above is also an issue for this analysis. Since these cases do not help us understand noise characteristics of the instrument, all granules centered south of 60 degrees south latitude are excluded from the analysis below.

For each of the 240 granules, a quick-look graphic is made with images of BT difference between Level-1B observations and PCA reconstructions for those channels that are flagged for reconstruction differences. Figure 14 shows the report for granule 2. This typical granule has 17 channels that meet the criteria for reporting.

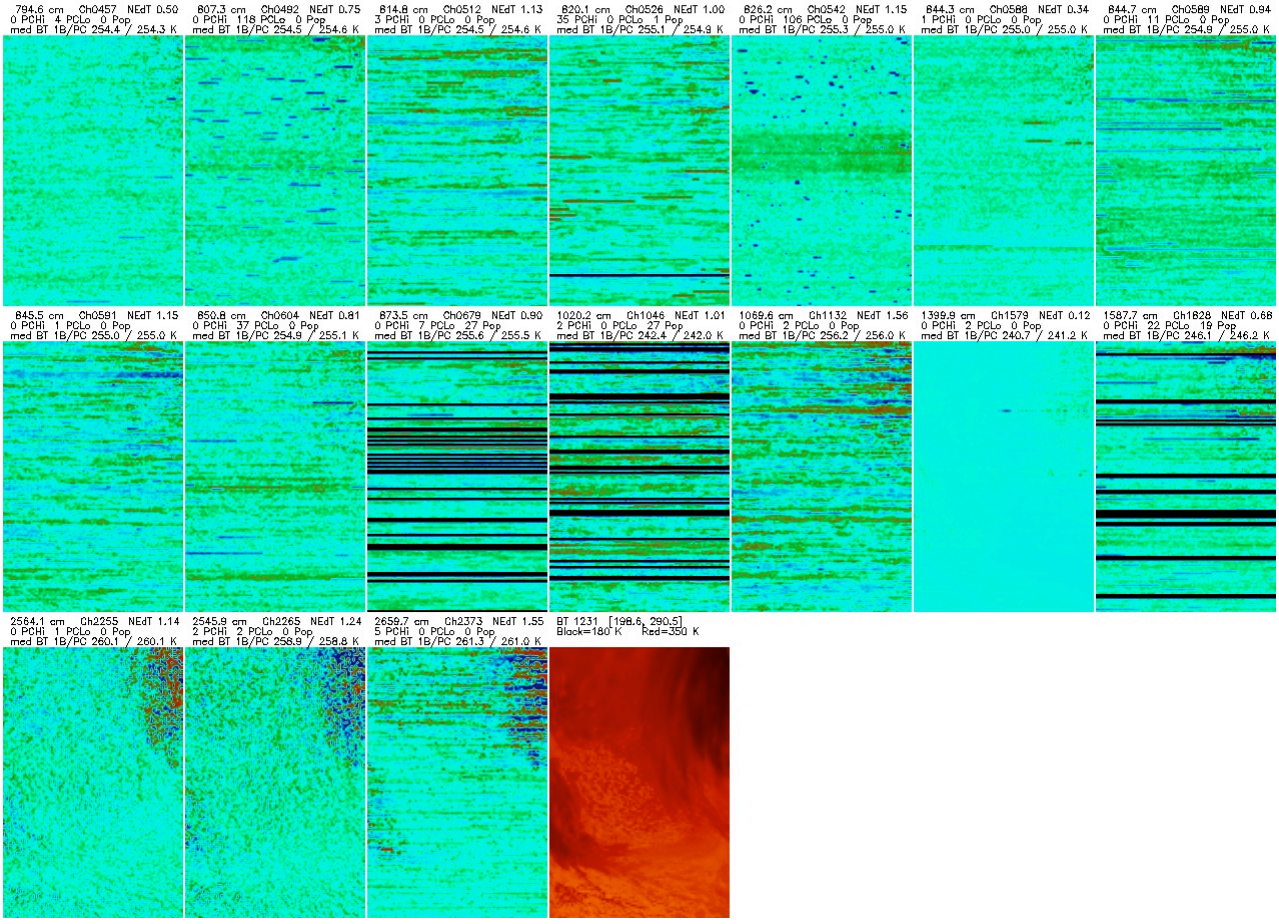

Figure 14 Per-channel images of differences between observed and reconstructed BTs, for all channels with at least one point of significant difference. Black stripes hide rows where the test is disabled because Level-1B detected a "pop" event.

The final red image shows the brightness temperature for this granule. The dark areas are cold clouds, and many shortwave channels are noisy in BT units in these areas. Because the test for

significance includes a check in radiance units, these are probably not the differences that trigger these channels being flagged.

Many of the images have a strong horizontal component. Because AIRS operates in a whisk-broom fashion, short-duration events show up as short horizontal lines. Errors in calibration from noise during calibration observations get smoothed over ~10 scans and so show up as more diffuse horizontal structures.

One of the primary non-Gaussian patterns encountered in AIRS data is "popping", where the baseline dark current from a detector suddenly shifts and some time later shifts back to its original level. The Level-1B algorithm detects these events when they are large and they last for several scans. In these cases Level-1C always cleans the channel and these are shown as black lines in figure 14. Most of the channels shown here have patterns that appear to be popping with short durations or small magnitude.

The most interesting case is channel 1579 (1399.9 cm^{-1}). It is a low noise channel (NEdT=0.12 K) where PCA and L1B agree very well except for 2 spectra in a row. This appears to be a radiation hit.

Except for the radiation hit case, all of these are channels which are known to have relatively high noise levels, but they were generally assumed to have Gaussian noise, so that they would be safe to use in climate applications where the noise will be reduced by averaging large numbers of data points. But since the noise now appears to be non-Gaussian, these channels should be avoided and Level-1C should clean them too.

Daily statistics show that these cases can be safely detected and flagged without significantly reducing the number of good channels. Figure 15 shows the noise levels of all channels, color coded by how often Level-1C already cleans them and how often the PCA test flags them as not matching expectations.

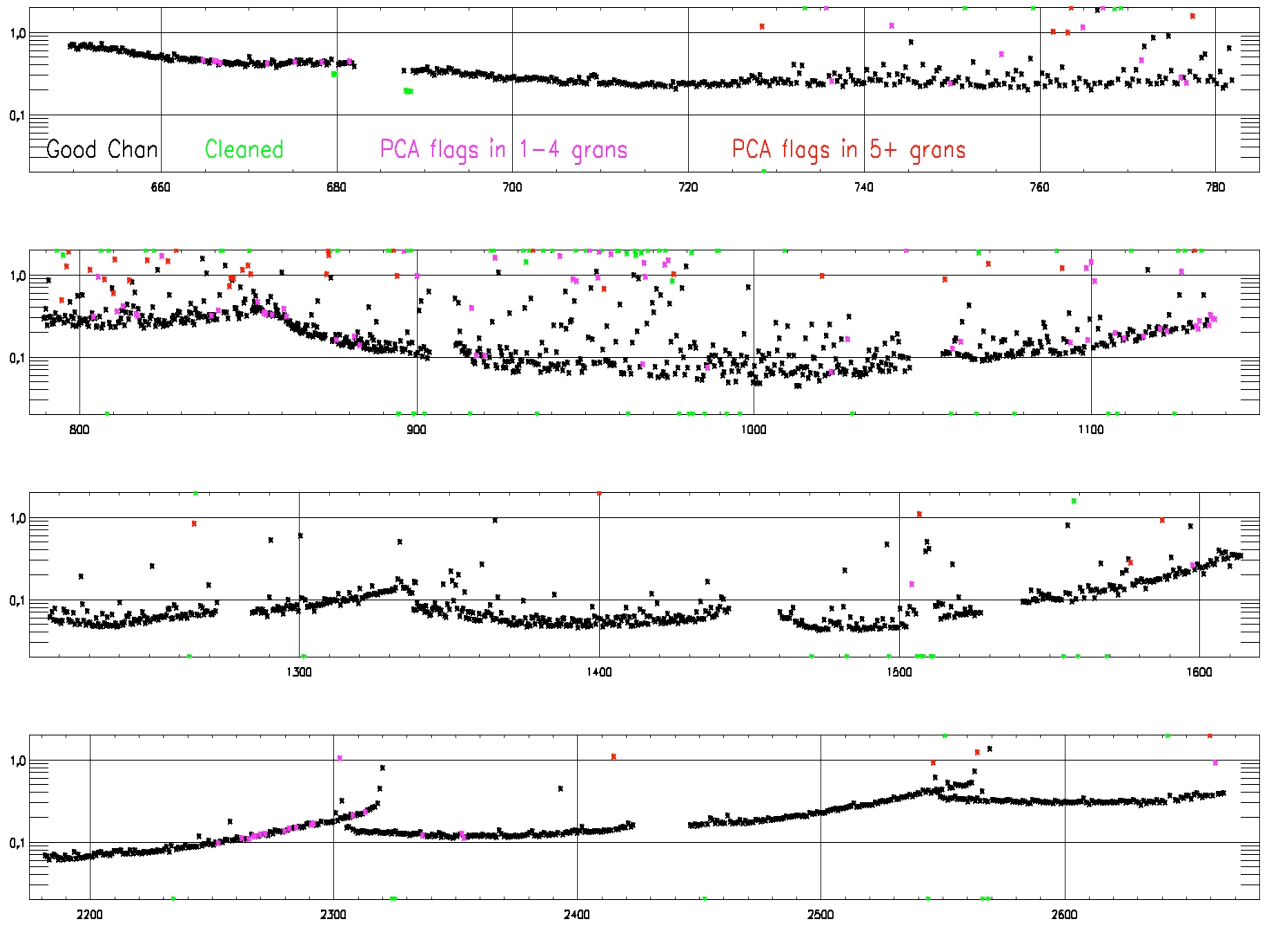

Figure 15 Daily maximum Noise Equivalent Delta Temperature (NEdT) (K) as a function of frequency (cm^{-1}) for all AIRS channels. Channels where only one of two detectors is used have their NEdT reduced by sqrt(2) to enhance the linear structure among the best channels. Colors show which channels were cleaned by Level-1C and which were not cleaned but had some 5K/5.7*NEN outliers with respect to PCA reconstruction.

In figure 15 we see that all channels with 5 or more granules containing significant differences between L1B observed radiances and PCA reconstruction have noise levels significantly higher than is common in neighboring channels. So it should be possible to craft a model of expected noise level per channel, and mark as questionable and/or replace with reconstructed values any channel with 2x (TBD) this level of noise.

There are a number of channels colored magenta among the best channels. These had only a few (usually 1) events. These events are likely radiation hits, so for these cases just the few affected measurements should be flagged and/or replaced.

With the existing L1C cleaning channel criteria, typically about 5% of channels are flagged as bad and filled for each granule. Adding a criterion replacing all channels with noise greater than 2x the value for the best neighboring channels would flag and clean an additional 5-10%. Users then would have very high confidence in the quality of the remaining 85-90% pristine channels, and would also have high quality substitute values for the 10-15% flagged channels.

There are many channels with noise over 2x the local baseline that are colored black in figure 15, indicating that no problems were detected with the PCA criteria. These could be good channels with slightly elevated but Gaussian noise, or they could have non-Gaussian noise at a magnitude

that is not detected. More investigation will be needed before tighter cleaning rules are implemented operationally.

For the remaining channels, PCA could be used to flag and replace the very rare radiation hits.

2.8 Using PCA reconstructed radiances to explore spatial misalignment in Level-1B

PCA reconstruction can also highlight spatial misalignment among channels. There are a small number of channels that see significantly more of one side or the other of an observed scene. The two most extreme among the channels that pass current quality screening are channels 2255 and 2265 at 2564.1 and 2545.9 cm^{-1} respectively. These are the last good channels at the near ends of two adjacent detector modules, and have their observation centroids displaced opposite directions along the cross-track (roughly east-west) axis. Note that because both of these channels have noise levels over 1 K, both of these channels would be

The PCA predicts with high accuracy what it expects an ideal detector at each frequency to see. The difference between what is actually observed and what PCA predicts functions as a sort of edge detection.

Figure 16a shows the brightness temperature at 1231 cm^{-1} for 2007-09-06 granule #108. This is a daytime granule with a lot of hot desert, cooler sea (the Red Sea in the center and the Mediterranean Sea at top), and cold clouds. Figures 16b and 16c show the almost complementary PCA residuals for channels 2255 and 2265. Coastlines and edges of clouds are the most prominent features.

While these two channels have high enough noise levels that they would already be replaced according to the scheme proposed in section 2.7, this does point out that PCA could be used to clean up more subtle misalignment artifacts in less-affected channels. The differences between PCA and L1B observations for other channels rarely or never rise to the 5 K level of significance used in the section 2.7 analysis, but these other channels might be cleaned only for scenes where large, oppositely signed PCA residuals in channels 2255 and 2265 show that spatial misalignment is an issue.

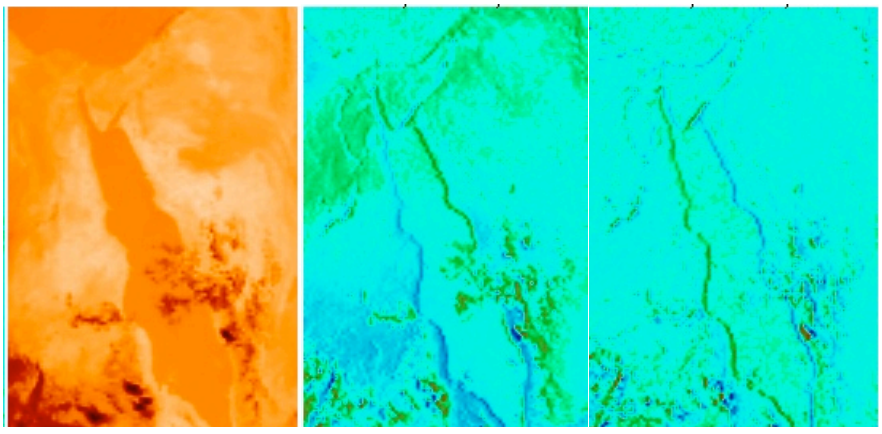

Figure 16 Daytime granule in Red Sea area. A) Brightness temperature at 1231 cm^{-1}. B) PCA residual for channel 2255. C) PCA residual for channel 2265

3. Spectrum Shift

The overall position of the AIRS channels are set with the grating model y-offset, which is an offset distance (micrometers) in the y-axis (dispersed) direction on the focal plane. This y-offset is added to the nominal y-position for the 2378 channels and then run through the AIRS grating model to generate channel frequencies.

Analysis of the AIRS radiances showed the channels were at -13.5 μm in September 2002 and November 2003. The grating model y-offset is calibrated to channel frequency for a reference grating temperature = 155.1325 K. But for unknown reason, at least two of the AIRS modules have shifted a little after launch, and the overall shift after launch is plotted in Figure 2. It shows that the frequency shift is not only seasonal dependent, but also latitude dependent. By regression analysis of the measured frequency shift from 2002 to 2010, the empirical prediction of the frequency shift has been determined by Strow and Hannon from UMBC (ref).

The frequency shift is about 8ppm in ten years, this could introduce 0.3K bias in brightness temperature. The changing frequency in L1B radiance data sets may cause certain confusion for users. Since the frequency shift is minor, we can determine the corrected spectrum using formula (4)

$$R = R_0 + \frac{dR}{d\nu} \cdot \Delta\nu \tag{4}$$

where R is the radiance at frequency ν after the frequency shift, R_0 is the spectrum before shift, $\Delta\nu$ represents the frequency shift amount, $\frac{dR}{d\nu}$ is the derivative of the spectrum at frequency ν. The $\frac{dR}{d\nu}$ is calculated from the grating model with different y-offset. The grating model provides two series of spectra with y-offset -14 μm and -15 μm respectively. Figure 13 shows the $\frac{dR}{d\nu}$ (y-axis) calculated for the shift from nominal -14 μm to -15 μm shift (black line), and for the shift from nominal -15 μm to -14 μm shift (blue line) verses the derivative calculated from the spline interpretation (x-axis). The linear fit to the data is expressed in formula (5), which shows the linear relationship between the calculated derivative and the derivative from spline interpretation. This relationship is critical to our frequency shift calculation since the slope or derivative is different for different spectrum, the spline derivative has to be calculated dynamically. Finally the shifted spectrum is shown in formula (6).

$$\frac{dR}{d\nu} = a\frac{dR^S}{d\nu} + b \tag{5}$$

$$R = R_0 + (a\frac{dR^S}{d\nu} + b) \cdot \Delta\nu \tag{6}$$

The shift parameters a and b are frequency dependent variables, their values for each channel are stored in the look up table.

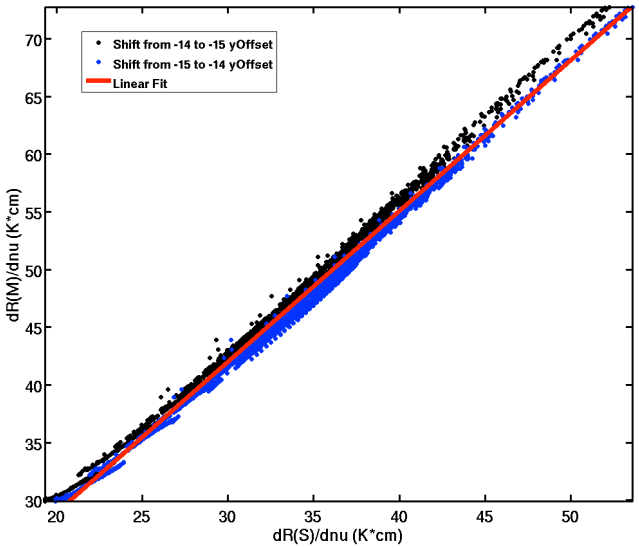

Figure 13. Scattering plot of the calculated spectrum derivative vs. the derivative from -14 µm to -15 µm shift (black line) and -15 µm to -14 µm shift (blue line). Red line is the linear fit to the data.

The model spectra are used to validate the algorithm. Figure 14 indicates that the averaged brightness temperature difference between shifted and true spectrum is much smaller around 5 mK as comparing to other algorithm with difference around 50 mK such as spline fit only. The distribution of the difference clearly shows that our algorithm is the best as comparing to spline re-sampling method and non-shift.

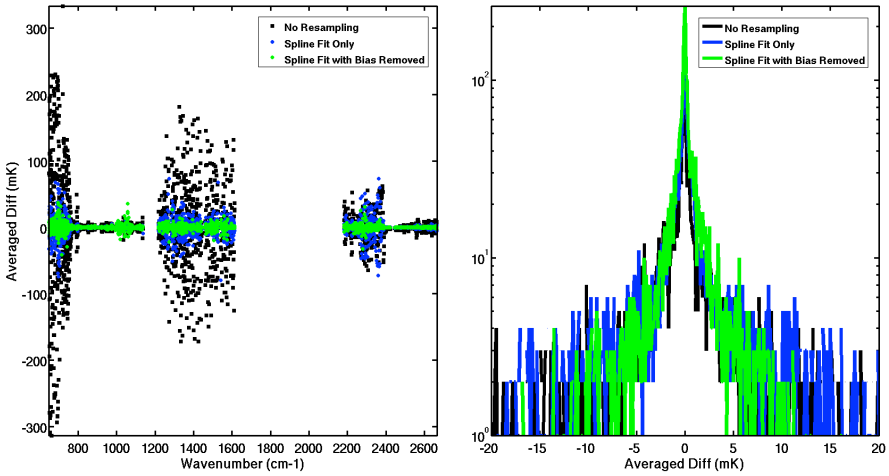

Figure 14. Averaged brightness temperature difference between shifted and original spectrum (left panel) and its distribution (right panel) of the brightness temperature vs. frequency from model spectra with no resampling (black dot or line), spline fit (blue dot or line), and spline fit with bias removed (green dot or line).

Figure 15 presents that the root mean square difference (RMS) of the brightness temperature between shifted and true spectrum is much smaller around 1 mK as comparing to the difference

around 10 mK for spline fit. The distribution of the difference also shows that our algorithm improve the final spectrum.

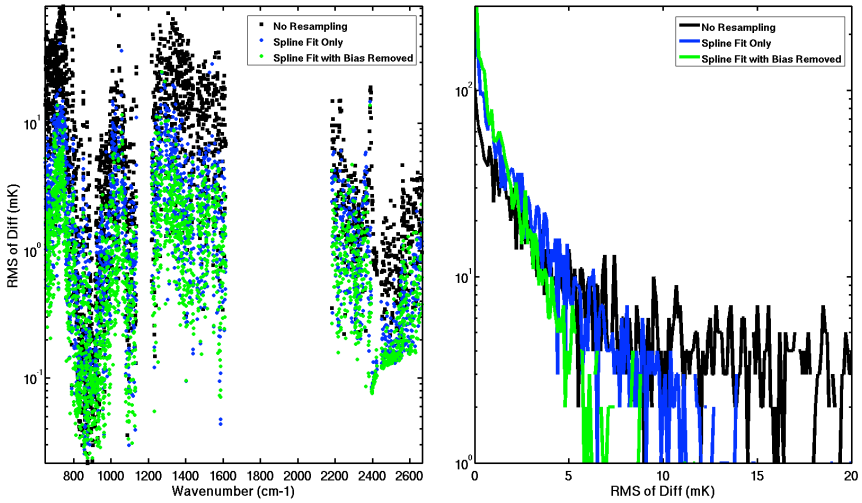

Figure 15. Root mean square difference (RMS) of the brightness temperature between shifted and original spectrum (left panel) and its distribution (right panel) of the brightness temperature vs. frequency from model spectra with no resampling (black dot or line), spline fit (blue dot or line), and spline fit with bias removed (green dot or line).

4. Spectrum Gap and Overlap Fill

UMBC has simulated the AIRS spectra without any gaps as shown in Figure 16 with a typical spectrum showing the filled gaps. The buddy-system algorithm as discussed in section 2.3 is used here to get the best-correlated channels for the gap channels. The principal component analysis from the full spectra training set is further applied to the gap-filled spectrum to identify the outliers and replace them by the corresponding reconstructed values. The overlap channels are also treated as gaps. The frequencies of the overlap channels are chosen to be the same as the module on the lower frequency side. There are 349 new gap channels, which are from the UMBC full spectra model. The new gap frequencies are listed in table 2. The total number of channels increases to 2660 after the gaps are filled.

Figure 17 shows the comparison of the overlap channels between modules M-01a and M-02a. The AIRS shadow channels are problematic and should be used with caution. The gap filled spectrum in the overlap region cleverly avoids the shadow channels in both modules as indicated in Figure 17. The overall statistics of the algorithm will be evaluated in section 5.

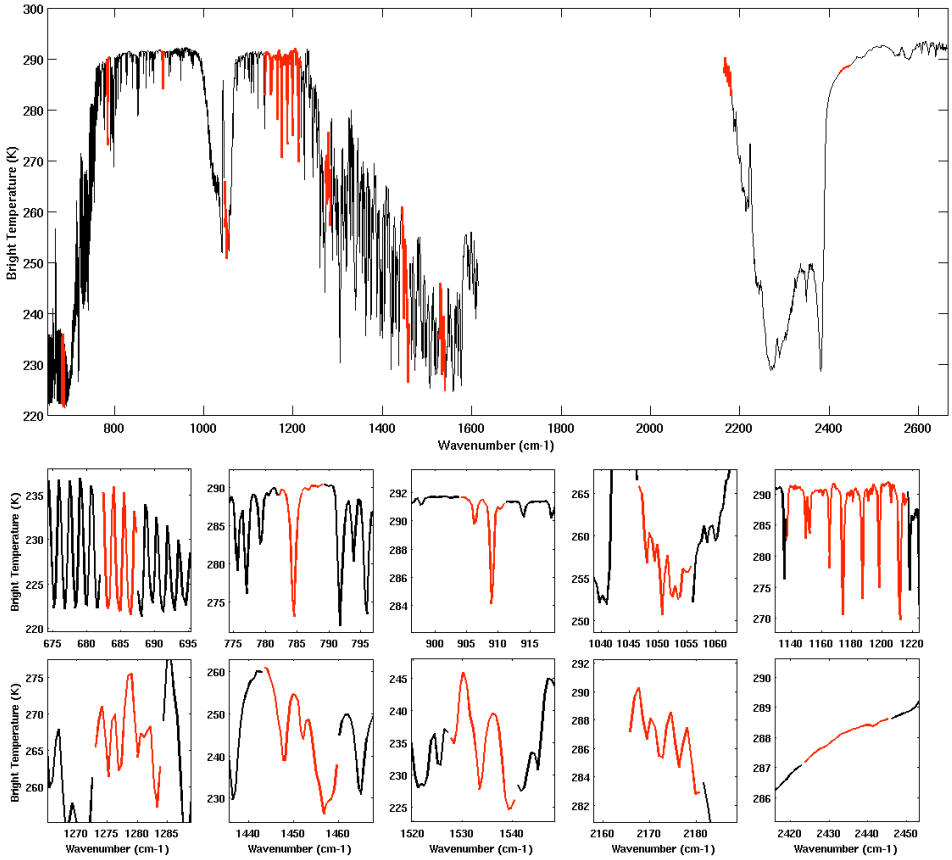

Figure 16. Sample spectrum from the full spectrum training set. The black lines represent the existing channels, and the red lines are the gap channels.

Table 2. AIRS L1C New Channel Frequency (cm^{-1})

Gap #1	Gap #2	Gap #3	Gap #4	Gap #5				Gap #6	Gap #7	Gap #8	Gap #9	Gap #10
682.25	782.22	904.12	1046.65	1137.16	1159.59	1182.03	1204.98	1273.13	1443.65	1527.65	2165.88	2423.83
682.51	782.56	904.46	1047.10	1137.68	1160.11	1182.55	1205.50	1273.66	1444.23	1528.29	2166.75	2424.80
682.76	782.89	904.80	1047.55	1138.20	1160.64	1183.07	1206.02	1274.20	1444.80	1528.93	2167.61	2425.78
683.02	783.23	905.14	1048.00	1138.73	1161.16	1183.59	1206.55	1274.73	1445.37	1529.57	2168.48	2426.75
683.27	783.56	905.48	1048.45	1139.25	1161.68	1184.11	1207.07	1275.27	1445.95	1530.21	2169.35	2427.72
683.53	783.90	905.82	1048.90	1139.77	1162.20	1184.63	1207.59	1275.80	1446.52	1530.85	2170.22	2428.70
683.78	784.23	906.15	1049.34	1140.29	1162.72	1185.16	1208.11	1276.34	1447.09	1531.49	2171.09	2429.67
684.04	784.57	906.49	1049.79	1140.81	1163.25	1185.68	1208.63	1276.87	1447.66	1532.14	2171.95	2430.64
684.29	784.90	906.83	1050.24	1141.33	1163.77	1186.20	1209.15	1277.40	1448.24	1532.78	2172.82	2431.61
684.54	785.24	907.17	1050.69	1141.86	1164.29	1186.72	1209.68	1277.94	1448.81	1533.42	2173.69	2432.59
684.80	785.58	907.51	1051.14	1142.38	1164.81	1187.24	1210.20	1278.47	1449.38	1534.06	2174.56	2433.56
685.05	785.91	907.85	1051.59	1142.90	1165.33	1187.76	1210.72	1279.01	1449.96	1534.70	2175.43	2434.53
685.31	786.25	908.19	1052.04	1143.42	1165.85	1188.29	1211.24	1279.54	1450.53	1535.34	2176.29	2435.50
685.56	786.58	908.53	1052.49	1143.94	1166.38	1188.81	1211.76	1280.08	1451.10	1535.98	2177.16	2436.48
685.82	786.92	908.87	1052.94	1144.46	1166.90	1189.33	1212.28	1280.61	1451.68	1536.62	2178.03	2437.45
686.07	787.25	909.21	1053.39	1144.99	1167.42	1189.85	1212.81	1281.15	1452.25	1537.26	2178.90	2438.42
686.33	787.59	909.54	1053.83	1145.51	1167.94	1190.37	1213.33	1281.68	1452.82	1537.90	2179.77	2439.40
686.58	787.92	909.88	1054.28	1146.03	1168.46	1190.89	1213.85	1282.22	1453.39	1538.54	2180.64	2440.37
686.84	788.26	910.22	1054.73	1146.55	1168.98	1191.42	1214.37	1282.75	1453.97	1539.18		2441.34
687.09	788.60	910.56	1055.18	1147.07	1169.51	1191.94	1214.89	1283.28	1454.54	1539.82		2442.31
687.35	788.93	910.90	1055.63	1147.59	1170.03	1192.46	1215.41	1283.82	1455.11	1540.46		2443.29
				1148.12	1170.55	1192.98	1215.94		1455.69			2444.26
				1148.64	1171.07	1193.50	1216.46		1456.26			2445.23
				1149.16	1171.59	1194.02	1273.13		1456.83			
				1149.68	1172.11	1194.55	1273.66		1457.41			
				1150.20	1172.64	1195.07	1274.20		1457.98			
				1150.72	1173.16	1195.59	1274.73		1458.55			
				1151.25	1173.68	1196.11	1275.27		1459.12			
				1151.77	1174.20	1196.63	1275.80		1459.70			
				1152.29	1174.72	1197.15	1276.34					
				1152.81	1175.24	1197.68	1276.87					

				1153.33	1175.77	1198.20	1277.40					
				1153.85	1176.29	1198.72	1277.94					
				1154.38	1176.81	1199.24	1278.47					
				1154.90	1177.33	1199.76	1279.01					
				1155.42	1177.85	1200.28	1279.54					
				1155.94	1178.37	1200.81	1280.08					
				1156.46	1178.90	1201.33	1280.61					
				1156.98	1179.42	1201.85	1281.15					
				1157.51	1179.94	1202.37	1281.68					
				1158.03	1180.46	1202.89	1282.22					
				1158.55	1180.98	1203.41	1282.75					
				1159.07	1181.50	1203.94	1283.28					
						1204.46	1283.82					

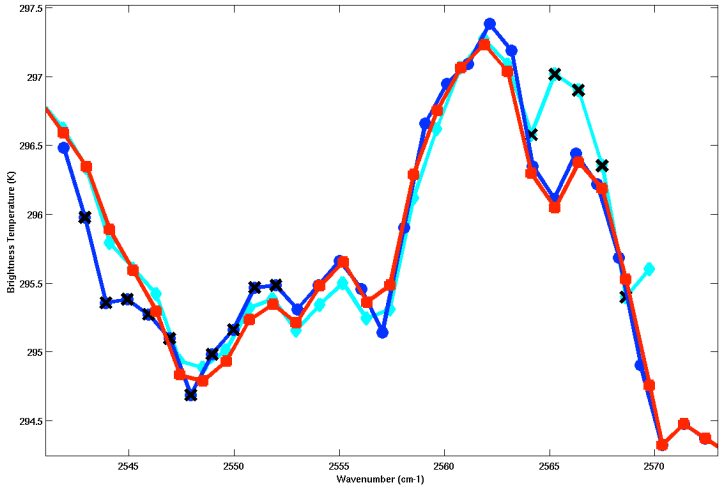

Figure 17. Overlap spectrum between modules M-01a (blue) and M-02a (cyan). The red line is the gap-filled spectrum and the black cross symbol represents the shadowed channels.

5. Validation Using IASI Spectra

We have used Infrared Atmospheric Sounding Interferometer (IASI) [Blumstein *et al*., 2007] data to validate the AIRS gap filling technique. IASI is a key payload element of the METOP-A series of European meteorological polar-orbit satellites launched in October 19, 2006. It is primarily designed for weather forecast and measures accurate temperature profiles in the troposphere and lower stratosphere (accuracy 1 K (RMS) at vertical resolution of 1km in the lower troposphere), as well as moisture profiles in the troposphere (10-15 % with 1-2 km vertical resolution). Technical details about IASI and applications for chemistry are explained by Clerbaux *et al*. [2009]. The measurement technique is based on passive IR remote sensing using an accurately calibrated Fourier Transform Spectrometer operating in the 3.7 - 15.5 µm spectral range and an associated infrared imager operating in the 10.3 - 12.5 µm spectral range. IASI has 8461 spectral samples, aligned in three bands between 645.0 cm^{-1} and 2760 cm^{-1} (15.5 µm and 3.63 µm) without gaps, with a spectral resolution of 0.5 cm^{-1} (FWMH) after apodization (L1C spectrum). The spectral sampling interval is 0.25 cm^{-1}. The IASI sounder is coupled with the IIS, which consists of a broadband radiometer measuring between 833 cm^{-1} and 1000 cm^{-1} (12µm and 10µm) with a high spectral resolution.

The one-day spectra measured by IASI over Atlantic Ocean are displayed in Figure 18, which covers variety of spectra. The spectrum is very noisy in short wavelength region; therefore we only use the spectrum in wavenumber less than 2200 cm^{-1}. Each IASI spectrum is resampled into AIRS spectrum frequency grid using spline interpolation, the radiance values of the L1C gap channels are also obtained by the spline interpolation from IASI spectra. The gap-fill algorithm then processes the resampled IASI spectra, and the averaged difference and its standard deviation in the gap regions are shown in Figure 19.

Figure 19 shows the spectra in the region 600 cm^{-1} to 1620 cm^{-1}. The high frequency part is not shown here since the anomalies of the IASI spectra could introduce some artifacts. The mean difference of the gap-filled region is within ±0.2K, and its standard deviation or scattering is within 0.1K. Further validation from other measurements will be investigated later.

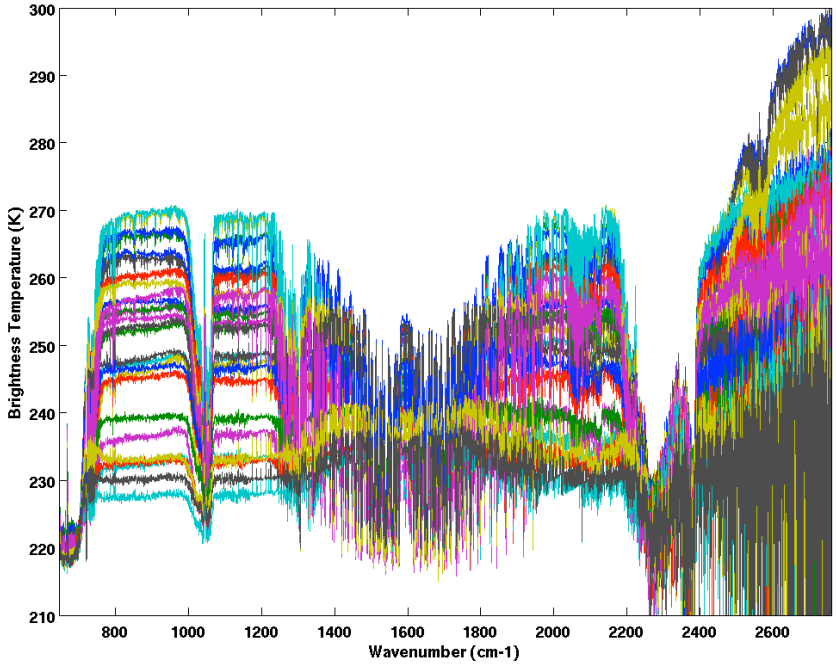

Figure 18. One-day measurements of the spectra by IASI over Atlantic Ocean.

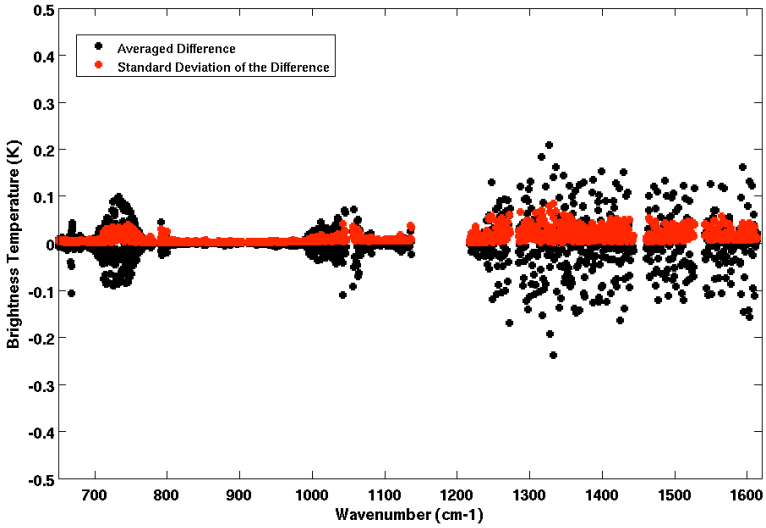

Figure 19. The averaged difference and standard deviation of the difference between the gap-filled spectra and the IASI spectra from one-day measurements over Atlantic Ocean.

6. PGE Execution Flow

(Need comments from Evan, need name and locations of all input tables)

The whole AIRS L1C software process consists of offline processing and inline processing parts. The task of offline process is to generate all necessary lookup tables for the inline process. The following summarizes the main offline processing steps for producing lookup tables for L1C cleaned spectrum process.

- Pre-process the clear sky model spectra to build the 'buddy' system and save the first ten best-correlated channels into a table.

- Pre-select true AIRS measured spectra and fill the dead and bad channels. The "buddy" system then is built up from these cleaned true spectra, and the PCA analysis performed on these true spectra too. The results are both saved into our L1C lookup table.

- Pre-calculate the frequency parameters *a* and *b* from the model spectra, and the results are stored in L1C lookup table.

- The "buddy" system is built up from the full spectrum training set provided by Scott Hannon. The results are both saved into our L1C lookup table. This lookup table is used for the gap filling and overlap channels modification.

The offline process flow chart is shown in Figure 20. It consists of three independent processes as indicated in three gray areas in Figure 20. The left area shows the generation of the lookup tables for the spectrum cleaning process, and the middle area is for the lookup table generation for

frequency shift process, and finally the right area shows the lookup table creation for the gap fill and overlap channels processing.

The following summarizes the main processing steps for producing L1C cleaned spectrum products, and the flow chart is shown in Figure 21.

- The first pass to clean the spectrum using "buddy' system.
- The second pass to reconstruct the spectrum using PCA, and the spectrum is then re-scanned for bad channels. The newly founded bad channels are filled with reconstructed value.
- The brightness temperature slope vs. frequency of each channel is then calculated, and the radiance is then calculated for the predicted channel frequency.
- Fill the gap and overlapped channels.
- Calculate the uncertainty estimates

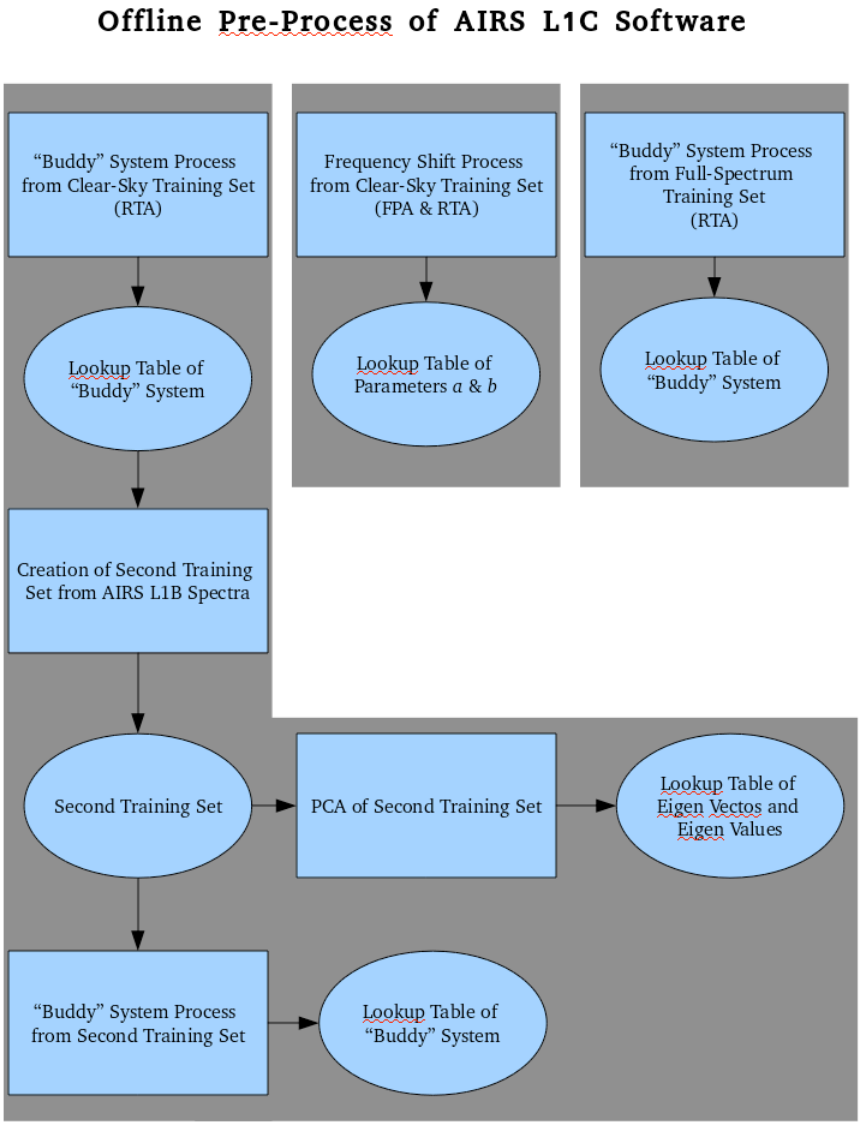

Figure 20. AIRS L1C software offline processing flow diagram.

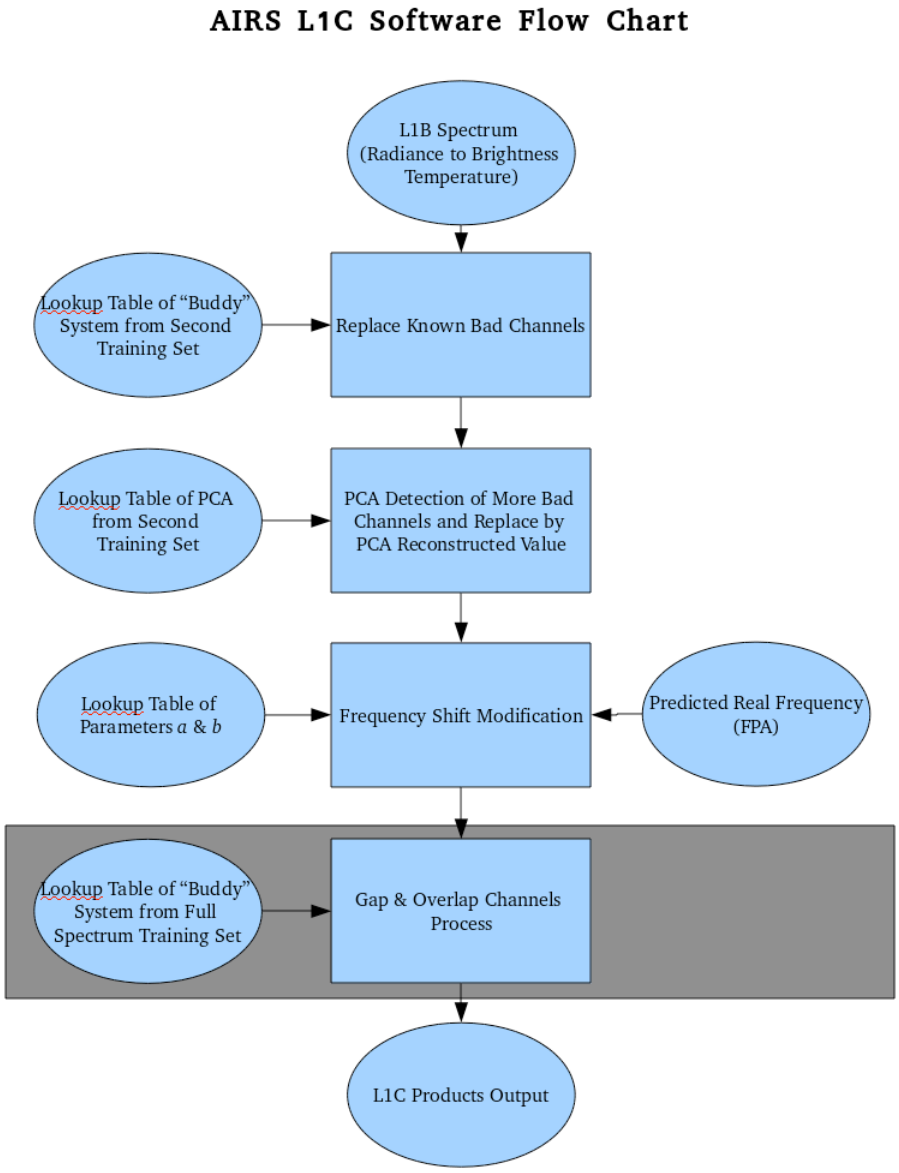

Figure 21. AIRS L1C software inline processing flow diagram.

7. Summary

An algorithm has been presented which can correct for the effect of time-variable non-Gaussian noise in AIRS spectra. This algorithm will be used as the basis for a new AIRS science data product—Level 1C—calibrated and cleaned radiances. That product will be made available to the public in a future version of the AIRS science software that runs at the GES DISC. Key features are the absence of interpolation, extrapolation, and resampling. Most channels have their calibrated radiances untouched from the basic product—Level 1B—calibrated radiances. The dead and bad channels have their radiances replaced by the "buddy" or the average of ten measured radiances from strongly correlated channels. This replacement process is performed independently for every spectrum. We have shown that replacement does not add significant bias and does not introduce

undue noise. The gap and overlapped channels are filled with the similar algorithm next per user's choice. The Level 1C product is not a substitute for Level 1B (which will remain the primary AIRS Level 1 product), but an enhancement for optional use by users.

The process described here involves two passes. The first pass is computationally cheap and the other is expensive. The "buddy" system algorithm is used in the first pass in both cleaning and gap-fill process. The PCA is computational expensive but affordable in the second pass. It is required in order to detect bad channels which have been slipped through the NEΔT check. There are also two arbitrary thresholds used. One is the local granule average NEΔT cutoff used in the first pass. The other is the difference threshold between the observed brightness temperature and the PCA reconstruction used in the second pass.

We expect that use of the fully complete Level 1C product will significantly enhance the utility of the AIRS instrument for climate studies. AIRS Level 1C data will be more easily cross-calibrated with other instruments. Some subtle instrument effects (such as very small frequency shifts) will be fully accounted for, reducing the likelihood that effects of an instrument feature could be misinterpreted as a climate trend.

References

Blumstein, D., B. Tournier, F. R Cayla, T. Phulpin, R. Fjo rtoft, C. Buil, and G. Ponce, In-flight performance of the infrared atmospheric sounding interferometer (IASI) on METOP-A, SPIE Conference, Vol 6684, San Diego (2007).

Chahine, M. T., T. S. Pagano, H. H. Aumann, R. Atlas, C. Barnet, L. Chen, M. Divakarla, E. J. Fetzer, M. Goldberg, C. Gautier, S. Granger, F. W. Irion, R. Kakar, E. Kalnay, B. H. Lambrigtsen, S. Y. Lee, J. Le Marshall, W. McMillan, L. McMillin, E. T. Olsen, H. Revercomb , P. Rosenkranz, W. L. Smith, D. Staelin, L. L. Strow, J. Susskind, D. Tobin and W. Wolf, The Atmospheric Infrared Sounder (AIRS): improving weather forecasting and providing new insights into climate, *Bulletin of the American Meteorological Society*, **87**, 891-894, DOI: 10.1175/BAMS-87-7-891 (2006)

Clerbaux, C., Boynard, A., Clarisse, L., George, M., Hadji-Lazaro, J., Herbin, H., Hurtmans, D., Pommier, M., Razavi, A., Turquety, S., Wespes, C., and Coheur, P.-F.: Monitoring of atmospheric composition using the thermal infrared IASI/MetOp sounder, *Atmos. Chem. Phys*., **9**, 6041–6054, doi:10.5194/acp-9-6041-2009 (2009).

Gaiser, S. L., Hartmut H. Aumann, L. Larrabee Strow, Scott E. Hannon, and Margaret Weiler, In-Flight Spectral Calibration of the Atmospheric Infrared Sounder, IEEE TRANSACTIONS ON GEOSCIENCE AND REMOTE SENSING, VOL. 41, NO. 2 (2003).

Jolliffe, I. T.,Principal Component Analysis. Springer-Verlag. pp. 487. doi:10.1007/b98835. ISBN 978-0-387-95442-4 (1986).

Strow, L. L., Scott E. Hannon, Margaret Weiler, Kenneth Overoye, Steven L. Gaiser, and Hartmut H. Aumann, Prelaunch Spectral Calibration of the Atmospheric Infrared Sounder (AIRS), IEEE TRANSACTIONS ON GEOSCIENCE AND REMOTE SENSING, VOL. 41, NO. 2 (2003)

Weiler , M. H., Kenneth R. Overoye, James A. Stobie, Paul B. O'Sullivan, Steven L. Gaiser, Steven E. Broberg, and Denis A. Elliott, Performance of the Atmospheric Infrared Sounder (AIRS) in the Radiation Environment of Low-Earth Orbit, SPIE International Symposium on Optical Science and Technology, Vol. 5882, San Diego (2005).